DESCRIPTION OF THE CANADIAN REGIONAL CLIMATE MODEL

D. CAYA[1], R. LAPRISE[1], M. GIGUÈRE[1], G. BERGERON[1],
J. P. BLANCHET[1], B. J. STOCKS[2], G. J. BOER[3] and N. A. McFARLANE[3]

[1]*Cooperative Centre for Research in Mesometeorology and Université du Québec à Montréal, CP 8888, Succursale Centre-Ville, Montréal Québec, H3C 3P8, Canada*
[2]*Forestry Canada, Ontario Region, Sault-Sainte-Marie, Ontario P6A 5M7, Canada*
[3]*Canadian Centre for Climate Modelling and Analysis, University of Victoria, British Columbia, Canada*

Abstract. Simulation of regional climate by limited-area model coupled with global low-resolution model is becoming a standard approach to achieve high-resolution climate projections at a computationally affordable cost. A regional climate model (RCM) based on a state-of-the-art numerical formulation is under development at the Université du Québec à Montréal. A brief description of this Canadian RCM (CRCM) is given. The characteristics of its dynamical formulation and the processes involved in its physical parameterisation are described. Results of a short simulation show that CRCM develops fine-scale features of climatological interest.

Keywords. MODEL, SIMULATION, REGIONAL, CLIMATE, MODELLING, GCM, RCM, LAM.

1. Introduction

Global general circulation models (GCMs) are the main tools available today for the simulation of climate. The very long integrations required for climate studies, however, impose a strong constraint on the maximum spatial resolution at which GCMs can be run. Half a day of supercomputer CPU time is needed for a one-year integration of a typical GCM with spatial resolution of the order of 300 km. This limited spatial resolution is currently identified as one of the major limitations in the ability of GCMs to properly simulate the hydrological cycle (IPCC, 1992). Because computing time required to run a GCM increases approximately with the third power of the horizontal grid resolution (fourth power if the concomitant vertical resolution is included), running a GCM at a resolution of the order of 30 km would require roughly two days of supercomputer computation per simulated day (Giorgi and Mearns, 1991). This spatial resolution would be required for a good representation of hydrology related processes. Since the computing power necessary for global fine-scale climate modelling will not be available in a near future, alternative approaches have to be explored.

Two major constraints are related to climate simulation: long integrations of the order of a few decades and global coverage of the Earth. One approach to refine the coarse resolution of GCMs consists in of limiting the spatial coverage of the high-resolution domain while maintaining global low-resolution coverage. In this approach, a high-resolution limited-area model (LAM) is nested in a low-resolution global model over the region of interest. Large-scale information from the global low-resolution model is transferred to the LAM by forcing its lateral boundaries with the values of the low-resolution global model. In this one-way nesting technique, the LAM receives its lateral boundary values from the outputs of the global model. This approach offers the

Water, Air and Soil Pollution **82**: 477–482, 1995.

possibility of increasing the horizontal resolution of climate models by nearly an order of magnitude while keeping the computational cost at an affordable level because the fine grid is of limited area. Regional climate simulation for limited area is then possible. The potential of regional climate modelling by nesting a high-resolution regional model in a lower resolution general circulation model (GCM) has been demonstrated in several papers by Giorgi (e.g., Giorgi *et al.*, 1993).

This paper is intended to give a brief description of a regional climate model (called the Canadian RCM or CRCM) currently under development at the Université du Québec à Montréal (UQAM). Preliminary results of a two-month integration are also presented to illustrate the ability of the model to represent regional-scale characteristics of some climatological fields.

2. Model Description

CRCM results from coupling the complete subgrid-scale parameterisation package of the second-generation Canadian GCM (GCMII, McFarlane *et al.*, 1992) with a very efficient dynamical model. This model, based on semi-Lagrangian and semi-implicit integration scheme, is the Cooperative Centre for Research in Mesometeorology's Mesoscale Compressible Community (CCRM-MC2) model (Bergeron *et al.*, 1994; Tanguay *et al.*, 1990). A one-way nesting procedure is used to drive the CRCM with GCMII data, i.e. CRCM gets information from GCMII through its lateral boundary, but it does not influence GCMII. Using GCMII as driving model for the CRCM permits both driving and driven models to share the same subgrid-scale parameterisation package, which facilitates the transfer of information between the two models. Another important advantage of using GCMII subgrid parameterisation is that all geophysical data files (soil type, vegetation, bare soil albedo, etc.) needed for physics parameterisation are global, and configuring the model for a specific area of the globe is thus simpler.

The current configuration of the model consists of a grid of 120 by 120 points covering a (5400 km)^2 area centred over the state of Vermont. The various fields are projected on a polar-stereographic grid with a resolution of 45 km at 60°N. In the vertical, 10 unequally spaced terrain-following Gal-Chen coordinate (Gal-Chen and Somerville, 1975) levels, from the ground up to 30 km, are used. Simulations with a 30-level version are also in progress. The following fields at the boundaries are driven by GCMII: wind components, temperature, pressure and water vapour. They are interpolated from GCMII archived data onto the CRCM lateral boundaries. Initial conditions are also taken from GCMII archived data. A sponge zone of ten gridpoints on the boundary of the domain is used to blend CRCM fields with the information received from GCMII. The nesting method used is inspired from that of Davies (1976) and refined by Robert and Yakimiw (1986) and Yakimiw and Robert (1990). Over a distance of ten gridpoints from the lateral boundaries, the variables of the regional model are gently and gradually blended with the those of the driving (global) model. By the time the CRCM lateral boundaries are reached, the values of the driving model variables are imposed. Throughout the rest of the grid (free zone), the variables of the regional model are not affected explicitly by those of the global model.

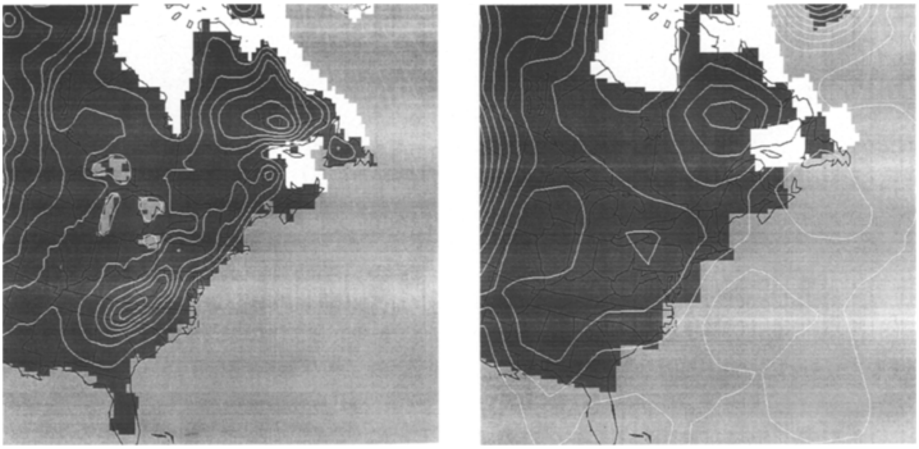

(a) (b)

Fig. 1. January land-sea-ice mask and topography of the 45 km CRCM (a) and T32 GCMII (b) over North-America. Land gridpoints appear in dark grey, open water in light grey and sea ice in white. Topographic contours are drawn at 100 m intervals. The spectral GCM is projected on a Gaussian latitude–longitude grid with a resolution of 3.75° × 3.75° and interpolated on the CRCM polar-stereographic grid for display (the distance between gridpoints on the Gaussian grid is approximately 450 km).

The dynamics of the CRCM are based on the complete non-hydrostatic Euler equations. Therefore, the dynamical formulation does not restrict spatial scales at which the model can be run. In fact, this model is used also at the millimetre scale for research on supersonic flow, at a few hundred metres for moist convection problems and at synoptic scales for weather forecasting. The integration of the complete Euler equations is made affordable by the efficiency of the three dimensional semi-Lagrangian semi-implicit integration scheme. The efficiency of the integration scheme also permits a 20-minute timestep at 45-km resolution, which is a very long timestep for non-hydrostatic numerical model at this resolution. For comparison, GCMII uses the same timestep with a transform Gaussian grid of approximately 450-km resolution and an Eulerian explicit model with 45-km resolution usually runs with a 90-second timestep.

The physical parameterisation package (imported from GCMII) takes into account the following processes: vertical turbulent fluxes of momentum, mountain-wave drag, radiation absorption and emission (solar and terrestrial) by the atmosphere and by the surface, release (absorption) of latent heat when condensation (evaporation) occurs, precipitation (solid and liquid), convection (dry and moist), variation of the surface albedo (defined for the two spectral bands and function of ground cover type, soil moisture, snow cover and snow age), cloud cover (evaluated from the prognostic water vapour and temperature fields), surface energy budget, soil moisture regime, vegetation and soil characteristics. The physical package of GCMII (and therefore CRCM) also includes a ocean mixed-layer model and a thermodynamic sea-ice model. For the experiment described in this paper, both of these models were turned off and climatological values of sea-surface temperature (SST) and ice-coverage were used.

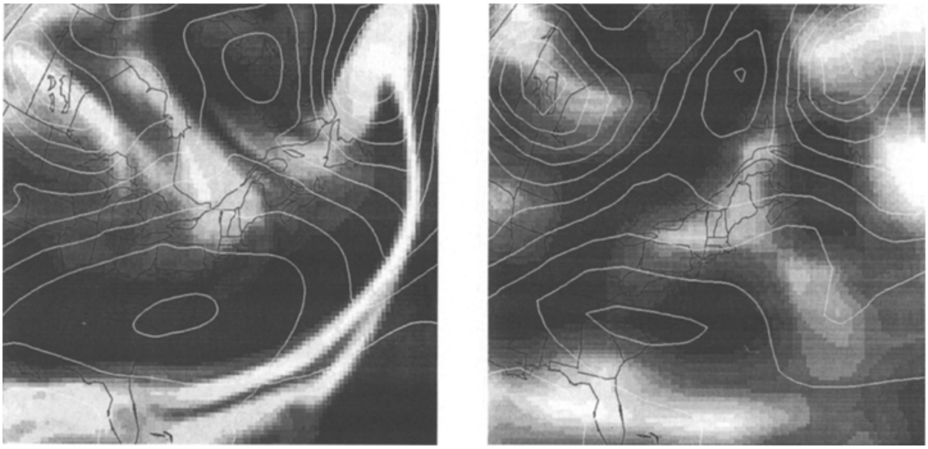

(a) (b)

Fig. 2. Relative humidity at 875 hPa and mean sea level (MSL) pressure for 14 January at 12Z for CRCM (a) and GCMII (b). Humidity field is presented in grey scale colour with dry area in black and wet area in white. MSL pressure contours are drawn at 4 hPa intervals. Minimum pressure in the cyclone over the East coast of Labrador are 985 hPa for CRCM and 987 hPa for GCMII.

3. Simulated Data and Discussion

The CRCM was integrated for a two-month period with the various model fields archived at six-hour intervals. The archived data for this experiment are time series of the following three dimensional fields: air temperature, pressure, water vapour, winds, clouds, and heating rates (solar and terrestrial). The following bi-dimensional surface fields are also archived: surface albedo, downward surface terrestrial radiation flux, solar flux absorbed at the surface, ground temperature, sensible heat flux, latent heat flux, precipitation, surface pressure, snow depth, liquid and frozen soil water contents.

Initial and CRCM time-dependent lateral boundary conditions were taken from archived files of a GCMII simulation that was initialised from January FGGE observed data. The CRCM simulation began the first day of the twelfth month (1 December of the first year) of a GCMII simulation. Sea surface temperature and ice cover are prescribed from climatological data. Average values of selected fields for the second month of the CRCM simulation (January) are here presented over a $(4500\text{ km})^2$ region excluding the nesting zone. It is important to note that a climatological analysis is not intended here, a two-month simulation being by no way long enough to have any statistical significance. The investigation was more directed onto the detection of regional characteristics in the various output fields of the CRCM compared to that of the driving GCM.

Figure 1 is used to highlight the differences between two model representations of the same world. Land-sea-ice mask of the 45-km resolution CRCM (a) and T32 (32 waves spectral model with roughly 450-km resolution) GCMII (b) over North America are shown. The spectral GCM is projected on a Gaussian latitude–longitude grid with a resolution of $3.75° \times 3.75°$. The Florida peninsula, the Great Lakes, James Bay and

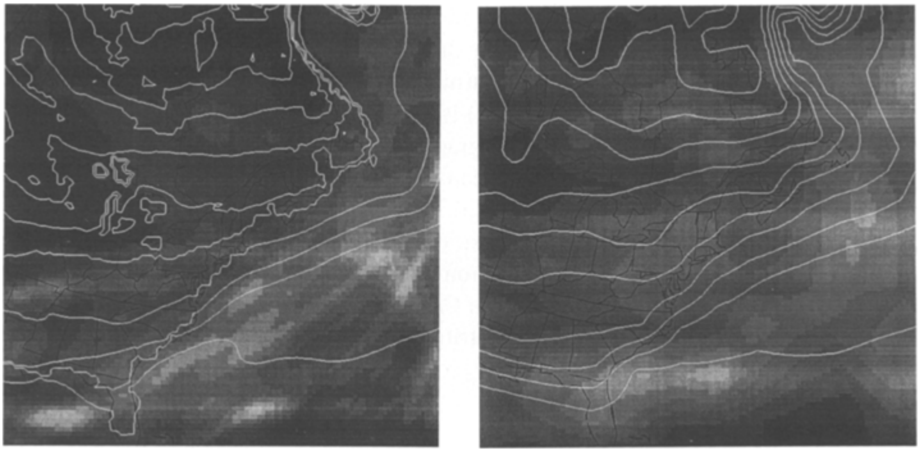

(a) (b)

Fig. 3. Monthly mean ground temperature and precipitation rate for CRCM (a) and GCMII (b). Monthly mean precipitation field is presented in grey scale colour with weak precipitation in black and strong precipitation in white. Ground temperature (and sea surface temperature over open water) contours are drawn at 5 °C intervals. Ground temperature on the Eastern side of the Florida peninsula is 23 °C in both CRCM and GCMII (SST are prescribed in both models).

other geographical characteristics of comparable (and smaller) scales cannot be reproduced at the coarse resolution of GCMII. The $1° \times 1°$ resolution of the reference file used to define the land-sea-ice mask of the CRCM is apparent in the finer details of the coastline. James Bay, Florida and the Great Lakes are now present in the model. Also on Figure 1, the topography of CRCM (a) and GCMII (b) are presented. Note that negative values are present over the ocean because of the spectral analysis made in GCMII. The increased resolution in CRCM allows a much more realistic representation of topography. In particular, sharper gradients are apparent in the Appalachian ridge and Labrador high lands, where maximum heights are almost twice as high as in the GCM.

It appears that even with a short simulation, many regional aspects of hydrology related fields (that are not well reproduced by a GCM) appear in the CRCM simulation. In particular, the classical comma shape in the distribution of humidity over a low-pressure system (located on the East coast of Labrador) is clearly visible in the CRCM output (Figure 2a); the coarse resolution GCMII (Figure 2b) cannot reproduce the strong gradient in the frontal zone. Mean sea level pressure is also contoured in white in Figure 2. Although the central pressure of the system is similar for both models (985 hPa for CRCM and 987 hPa for GCMII), the configuration of the cyclone is different. Again, the frontal zone in CRCM shows stronger gradients. This kind of structure in the CRCM humidity field develops rapidly after the initiation of a CRCM simulation. In order to evaluate the time needed by the CRCM to modify the humidity field from the patchy GCMII distribution to the more structured CRCM field, an experiment was conducted in which CRCM was initialised with GCMII data at a time when a deep cyclone was located over the area covered by the CRCM grid. It was observed that the frontal zone begins its development during the first 12 hours of CRCM simulation. After 48 hours, the observed CRCM distribution is attained.

The monthly mean precipitation and surface temperature for this single January CRCM simulation are presented in Figure 3a and corresponding fields for GCMII are presented in Figure 3b. The relative warm surface temperature of the Great-Lakes (with respect to surrounding temperatures) is clearly apparent in the CRCM field. One can also observe the strong temperature gradient over the ice edge near the Labrador coast. The distribution of the monthly mean precipitation rate is, again, more detailed in the CRCM than that simulated by the GCMII. The sharper definition of the various storm tracks that affected the east coast of North America within the month are apparent in the monthly mean precipitation field. The maximum mean precipitation rate observed is approximately 8 mm d^{-1} in CRCM and 7 mm d^{-1} in GCMII. Despite the similarity in the maximum values, the distributions are very different with much larger gradient in the CRCM.

4. Conclusion

These preliminary CRCM results demonstrate the ability of the nesting technique for the simulation of regional characteristics of the atmospheric flow. All the differences between simulations of the GCMII and the CRCM are directed toward what is expected for regional climate. A more detailed analysis of the performance of CRCM will be presented in Caya and Laprise (1995). Quantitative validation over much longer period of time, however, will be necessary to assess the performance of CRCM for regional climate simulation. These long integrations are now in progress and will be reported in later publications.

References

Bergeron, G., Laprise, R. and Caya, D.: 1994, *Formulation of the Mesoscale Compressible Community (MC2) Model.* Internal Report from Cooperative Centre for Research in Mesometeorology, Montréal, Canada, 165 pp.

Caya, D. and Laprise, R.: 1995, The Canadian Regional Climate Model. (Unpublished manuscript).

Davies, H. C.: 1976, *Quart. J. Roy. Met. Soc.* **102**, 405-418.

Gal-Chen, T. and Sommerville, R. C.: 1975, *J. Comput. Phys.* **17**, 209-228.

Giorgi, F., Bates, G. T. and Nieman, S. J.: 1993, *J. Climate* **6**, 75-95.

Giorgi, F. and Mearns, L. O.: 1991, *Rev. Geophys.*, **29**, 191-216.

Houghton, J. T., Jenkins, G. J. and Ephraums J. J.: 1990 (eds.), *Climate Change, the IPCC Scientific Assessment.* Intergovernmental Panel on Climate Change, Cambridge University Press, Cambridge, UK, 365 pp.

McFarlane, N. A., Boer, G. J., Blanchet J. P. and Lazarre, M.: 1992, *J. Climate*, **5**, 1013-1044.

Robert, A. and Yakimiv, E.: 1986, *Atmos.-Ocean*, **24**, 369-385.

Tanguay, M., Robert, A. and Laprise, R.: 1990, *Mon. Wea. Rev.* **118**, 1970-1980.

Yakimiv, E. and Robert, A.: 1990, *Atmos.-Ocean* **28**, 466-472.